Pergamon

Bioorganic & Medicinal Chemistry 6 (1998) 1695–1705

BIOORGANIC & MEDICINAL CHEMISTRY

Impact of Mixed-backbone Oligonucleotides on Target Binding Affinity and Target Cleaving Specificity and Selectivity by *Escherichia coli* RNase H

Ling X. Shen,* Ekambar R. Kandimalla and Sudhir Agrawal †

Hybridon, Inc., 620 Memorial Drive, Cambridge, MA 02139, USA

Received 2 February 1998; accepted 9 April 1998

Abstract—All phosphorothioate mixed-backbone oligonucleotides (MBOs) composed of deoxyribonucleotide and 2′-*O*-methylribonucleotide segments were studied for their target binding affinity, specificity, and RNase H activation properties. The 2′-*O*-methylribonucleotide segment, which does not activate RNase H, serves as a high affinity target-binding domain and the deoxyribonucleotide (DNA) segment, which binds to the target with a lower affinity than the former domain, serves as an RNase H-activation or target-cleaving domain. In order to understand the influence of the size and position of the DNA segment of MBOs on RNase H-mediated cleavage of the RNA target, we designed and synthesized a series of 18-mer MBOs with the DNA segment varying from a stretch of two to eight deoxyribonucleotides in the middle, at the 5′-end, or at the 3′-end of the MBOs. UV absorbance melting experiments of the duplexes of the MBOs with the complementary and singly mismatched RNA targets suggest that the target binding affinity of the MBOs increases as the number of 2′-*O*-methylribonucleotides increases, and that the binding specificity is influenced by the size and position of the DNA segment. Analysis of RNase H assay results indicates that the minimum substrate cleavage site and cleavage efficiency of RNase H are influenced by the position of the DNA segment in the MBO sequence. RNA cleavage efficiency decreases as the position of the DNA segment of the MBO·RNA heteroduplex is changed from the 3′-end to the middle and to the 5′-end of the target strand. Studies with singly mismatched targets indicate that the RNase H-dependent point mutation selectivity of the MBOs is affected by both the position and size of the DNA segment in the MBO sequence.

Introduction

Phosphodiester (PO) and phosphorothioate (PS) oligodeoxynucleotides have been shown to direct efficient cleavage of accessible complementary sequences of RNA in the presence of prokaryotic or eukaryotic RNase H.[1–6] PO-oligonucleotides activate RNase H better than the PS-oligonucleotides upon binding to the RNA target, possibly because of higher duplex stability between RNA and PO-oligonucleotide and/or higher binding affinity of PS-oligonucleotide to RNase H, inhibiting its catalytic activity at higher PS concentrations.[3,7] Recently, mixed-backbone oligonucleotides (MBOs) composed of a PO- or PS-segment flanked on both sides by nucleotide residues with modified sugar and/or phosphate moieties have been shown to improve target binding specificity, affinity, in vivo stability and biological activity.[6,8–14] In such mixed-backbone oligonucleotide constructs, the PO- or PS-deoxyribonucleotide segment serves as an RNase H activation domain and confines RNase H-mediated cleavage to limited sites on the RNA target; the segment with backbone modification does not activate RNase H and serves solely as a target-binding domain to ensure effective hybridization. In earlier studies, biophysical, biochemical and biological properties of MBOs containing segments of PO-oligonucleotides and methylphosphonate linkages were characterized.[12,15–17] Incorporation of

Key words: Antisense; mixed-backbone oligonucleotides; 2′-*O*-Me-RNA; RNase H cleavage specificity; point mutations.

*Present address: Variagenics, Inc., One Kendall Square, Building 400, Cambridge, MA 02139, USA

†Corresponding author. Tel: 508 482 7530; Fax: 508 482 7692; E-mail: sagrawal@hybridon.com

0968-0896/98/$—see front matter
PII: S0968-0896(98)00131-X

methylphosphonate linkages generally decreased the duplex stability, and moreover, PO-linkages in such MBOs were degraded by nucleases.[2,12,15–17] To design MBOs that have higher affinity for target RNA and are also stable against nucleases, we studied PS-MBOs, which have segments of deoxyribonucleotides and 2′-*O*-methylribonucleotides. This type of MBOs showed increased stability in vivo, and are more effective than PS-oligonucleotides in their biological activity both in vitro and in vivo.[6,8–14] The study described here was carried out to further understand the effect of the size, and position of the DNA segment of the MBOs on the duplex thermodynamic stability, RNase H-mediated cleavage of the target RNA, and selectivity towards singly mismatched target sequences using *Escherichia coli* RNase H as a model enzyme. *E. coli* RNase H has been better characterized than eukaryotic RNases H for its substrate affinity and specificity, and kinetics of catalysis.[12,18–20] Studies with purified *E. coli* RNase H and eukaryotic cell extracts, containing RNase H suggested that both prokaryotic and eukaryotic enzymes exhibit similar cleavage properties.[3,17]

Results

Design of mixed-backbone oligonucleotides (MBOs)

Phosphorothioate MBOs, composed of deoxyribonucleotide (DNA) and 2′-*O*-methylribonucleotide segments, were used in order to study the effect of such MBOs on RNase H-dependent scission of target RNA, and the specificity and selectivity of the MBOs. The 2′-*O*-methylribonucleotide segment in an MBO serves as a target-binding domain that contributes to the binding affinity of the MBO to the RNA target but does not activate RNase H. The DNA segment serves as an RNase H-activating domain that directs RNase H to cleave the RNA target within the target RNA sequence complementary to the DNA segment of the MBO.

In order to understand the effect of size and position of the DNA segment of MBOs on RNase H activation and target-point-mutation selectivity, we designed three sets of 18-mer MBOs with the DNA segment placed in the middle (M-set), at the 5′-end (5P-set) or at the 3′-end (3P-set) of the 18-mer sequence (Fig. 1). The length of the DNA segment varied from two to eight nucleotides, with the 2′-*O*-methylribonucleotide segment length adjusted accordingly to keep the overall length of the MBOs fixed (18-mer). To assess the selectivity of MBOs, four 30-mer RNA targets were synthesized. These included a matched target (RT) with its 18 central bases complementary to the MBO sequence, and three singly mismatched targets with a mismatched base positioned in the middle (RTM), near the 5′-end (RT5P), or near the 3′-end (RT3P) of the hybridization region of the target sequence. Nucleotide sequences and backbone constructs of the MBOs used in the study are shown in Tables 1–4 along with sequences of the four RNA targets, and a control phosphorothioate oligodeoxynucleotide (ODN).

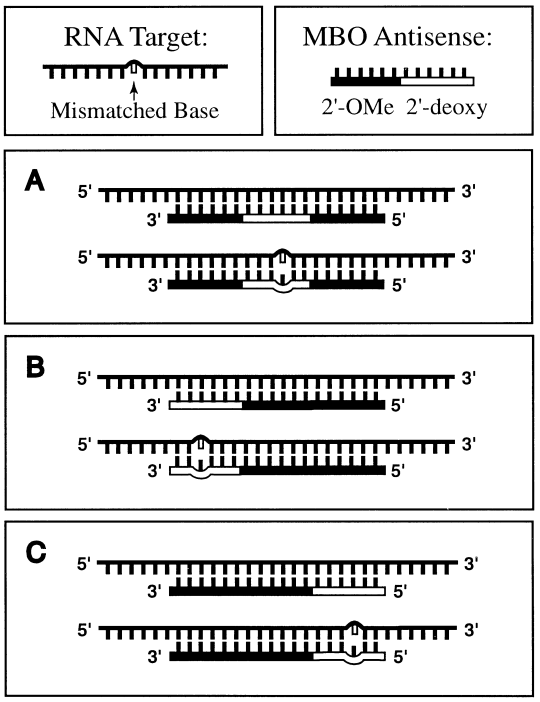

Figure 1. The mixed-backbone oligonucleotides (MBOs) used in the study as shown in panels A, B, and C with the 2′-deoxyribonucleotide segment positioned in the middle, and at the 3′- and 5′-ends of the MBO sequence, respectively. The length of the deoxyribonucleotide segment varies from two to eight nucleotide residues.

Differential binding affinity of MBOs for complementary and singly mismatched RNA targets

The melting temperature (T_m) of the MBO·RNA heteroduplexes was measured using UV absorbance melting experiments. The differential binding affinity of M-, 3P- and 5P-sets of MBOs for matched (RT) and singly mismatched (RTM, RT5P, or RT3P) RNA targets was evaluated from the T_m values determined from the UV absorbance melting curves. Tables 1–4 list the T_m values measured for the duplexes of MBOs as well as those of the control ODN with the four RNA (complementary and mismatched) targets.

The duplex of the control ODN with the RNA target (RT) showed a T_m of 61.5 °C. The binding affinity of

control ODN for the three mismatched RNA targets is in the order ODN·RT5P > ODN·RT3P > ODN·RTM (Table 1).

All MBO·RNA duplexes studied have T_ms higher than the duplexes of the control ODN (Tables 2–4). The T_m values for complementary MBO·RT heteroduplexes ranged from 73 to 81 °C. These T_m values reflect that the complementary MBO·RT heteroduplexes are thermodynamically more stable (12–20 °C) than the complementary ODN·RT heteroduplex. The increased thermodynamic stability of the MBO·RT heteroduplexes can be attributed to the 2′-*O*-methyl modification of the MBOs that confines the modified sugars in the 3′-*endo* conformation, favoring an A-form geometry for the heteroduplex.[9,21–25] The T_m values for the singly mismatched MBO·RNA duplexes ranged from 64 °C to 80 °C. By comparing the T_m values of the three sets of complementary duplexes with the same DNA window size, we observed the following trend in T_m: $T_m(M{\cdot}RT) \approx T_m(3P{\cdot}RT) > T_m(5P{\cdot}RT)$. A different trend in T_m was observed for singly mismatched duplexes: $T_m(3P{\cdot}RT5P) > T_m(5P{\cdot}RT3P) > T_m(M{\cdot}RTM)$. Within each set of the MBOs, the thermodynamic stability of the MBO·RT duplexes increased as the number of 2′-*O*-methylribonucleotide residues increased. The same correlation was also observed within each set of singly mismatched MBO·RNA duplexes.

The differential binding affinity of an oligonucleotide for the singly mismatched and matched RNA targets is evaluated by ΔT_m, the difference between the T_m values of the mismatched and matched heteroduplexes (Tables 1–4). A more negative ΔT_m (or a greater $|\Delta T_m|$) would be desired for a better target binding selectivity. For the heteroduplexes containing the control ODN, approximately a threefold increase in $|\Delta T_m|$ was observed as the position of single mismatch changed

Table 1. UV absorbance melting temperatures of ODN·RNA duplexes

Target/ODN[a]	Sequence	T_m(°C)[b]	ΔT_m(°C)[c]
ODN	CGGTCACTCCTCCGTGCG-5′		
RT	5′-ACCGCCGCCAGUGAGGAGGCACGCAGCCUU	61.5	
RTM	5′-ACCGCCGCCAGUGAG**U**AGGCACGCAGCCUU	45.8	−15.7
RT5P	5′-ACCGCCGC**A**AGUGAGGAGGCACGCAGCCUU	56.8	−4.7
RT3P	5′-ACCGCCGCCAGUGAGGAGGCAA**G**CAGCCUU	47.8	−13.7

[a]The control ODN is an 18-mer phosphorothioate oligodeoxyribonucleotide. The RNA targets are named according to the position of the mismatched base: RT represents the complimentary target; RTM, RT5P and RT3P represent the mismatched targets with a mismatched base present in the middle, near the 5′-end and 3′end of the RNA sequence, respectively. The mismatched base is shown in boldface.
[b]T_m determined from curve fits of the UV absorbance versus temperature profiles using a two-state transition model.
[c]$\Delta T_m = T_m$(mismatched duplex) $- T_m$(matched duplex).

Table 2. UV absorbance melting temperatures of MBO·RNA duplexes

Target/MBO[a]	Sequence	T_m(°C)[b]	ΔT_m(°C)[c]
RT	5′-ACCGCCGCCAGUGAGGAGGCACGCAGCCUU		
M2	CGGUCACUCCUCCGUGCG-5′	80.6	
M3	CGGUCACUCCTCCGUGCG-5′	79.6	
M4	CGGUCACTCCTCCGUGCG-5′	79.2	
M6	CGGUCACTCCTCCGUGCG-5′	76.9	
M8	CGGUCACTCCTCCGUGCG-5′	74.8	
RTM	5′-ACCGCCGCCAGUGAG**U**AGGCACGCAGCCUU		
M2	CGGUCACUCCUCCGUGCG-5′	71.0	−9.6
M3	CGGUCACUCCTCCGUGCG-5′	69.7	−9.9
M4	CGGUCACTCCTCCGUGCG-5′	68.1	−11.1
M6	CGGUCACTCCTCCGUGCG-5′	66.3	−10.6
M8	CGGUCACTCCTCCGUGCG-5′	64.3	−10.5

[a]The 2′-*O*-methyl/deoxyribonucleotide mixed-backbone oligonucleotides (MBOs)(M2-M8) are named according to the position (M for middle) and number (2–8) of deoxyribonucleotide residues (underlined). The RNA RT and RTM are as defined in Table 1. The mismatched base is shown in boldface.
[b]T_m determined from curve fits of the UV absorbance versus temperature profiles using a two-state transition model.
[c]$\Delta T_m = T_m$(mismatched duplex) $- T_m$(matched duplex).

from near the 3′-end of ODN to the middle or near the 5′-end of ODN. It should be noted that the observed $|\Delta T_m|$ difference between the two end-mismatched duplexes is due partly to the presence of secondary structures in the RNA targets. For the heteroduplexes containing the MBOs, ΔT_m became more negative as the position of the single mismatch changed from near the 3′-end to the 5′-end, and to the middle of the MBO sequence.

Antisense-dependent RNase H digestion of matched and singly mismatched RNA targets

At a 30-mer RNA target concentration of 33 nM, titration with the 18-mer control ODN showed significant inhibitory effect on *E. coli* RNase H activity at ODN concentrations greater than 20-fold of the target (data not shown). Therefore, 330 nM of oligonucleotides in a tenfold excess of the target was used in the RNase H assay to ensure full hybridization of the RNA targets while keeping the inhibitory effect of phosphorothioate ODN and MBOs on RNase H at a minimum. The target-point-mutation selectivity of the M-, 3P- and 5P-sets of MBOs was examined by hybridizing each of the MBOs to a matched (RT) or a singly mismatched (RTM, RT5P, or RT3P) RNA target and by comparing the extent of target cleavage in the presence of *E. coli* RNase H. Since the 2′-*O*-methylribonucleotide segments of MBOs do not activate RNase H, by narrowing the

Table 3. UV absorbance melting temperatures of MBO·RNA duplexes

Target/MBO[a]	Sequence	T_m(°C)[b]	ΔT_m(°C)[c]
RT	5′-ACCGCCGCCA**G**UGAGGAGGCACGCAGCCUU		
3PT	CGGUCACUCCUCCGUGCG-5′	81.4	
3P4	CGGTCACUCCUCCGUGCG-5′	79.4	
3P5	CGGTCACUCCUCCGUGCG-5′	79.4	
3P6	CGGTCACUCCUCCGUGCG-5′	77.9	
3P7	CGGTCACUCCUCCGUGCG-5′	76.4	
3P8	CGGTCACTCCUCCGUGCG-5′	75.5	
RT5P	5′-ACCGCCGC**AA**GUGAGGAGGCACGCAGCCUU		
3P2	CGGUCACUCCUCCGUGCG-5′	79.7	−1.7
3P4	CGGTCACUCCUCCGUGCG-5′	78.6	−0.8
3P5	CGGTCACUCCUCCGUGCG-5′	77.7	−1.7
3P6	CGGTCACUCCUCCGUGCG-5′	76.3	−1.6
3P7	CGGTCACUCCUCCGUGCG-5′	75.2	−1.2
3P8	CGGTCACTCCUCCGUGCG-5′	74.1	−1.4

[a]The 2′-*O*-methyl/deoxyribonucleotide mixed back-bone oligonucleotides (MBOs) (3P2-3P8) are named according to the position (3P for 3 prime) and number (2–8) of deoxyribonucleotide residues (underlined). The RNA RT and RT5P are as defined in Table 1. The mismatched base is shown in boldface.
[b]T_m determined from curve fits of the UV absorbance versus temperature profiles using a two-state transition model.
[c]$\Delta T_m = T_m$(mismatched duplex) $- T_m$ (matched duplex).

Table 4. UV absorbance melting temperatures of MBO·RNA duplexes

Target/MBO[a]	Sequence	T_m(°C)[b]	ΔT_m(°C)[c]
RT	5′-ACCGCCGCC**A**GUGAGGAGGCACGCAGCCUU		
5P4	CGGUCACUCCUCCGTGCG-5′	77.4	
5P5	CGGUCACUCCUCCGTGCG-5′	77.8	
5P6	CGGUCACUCCUCCGTGCG-5′	75.3	
5P7	CGGUCACUCCUCCGTGCG-5′	73.3	
RT3P	5′-ACCGCCGCC**A**GUGAGGA**G**GCA**A**GCAGCCUU		
5P4	CGGUCACUCCUCCGTGCG-5′	73.6	−3.8
5P5	CGGUCACUCCUCCGTGCG-5′	73.6	−4.2
5P6	CGGUCACUCCUCCGTGCG-5′	71.0	−4.3
5P7	CGGUCACUCCUCCGTGCG-5′	68.4	−4.9

[a]The 2′-*O*-methyl/deoxyribonucleotide mixed back-bone oligonucleotides (MBOs) (5P4-5P7) are named according to the position (5P for 5 prime) and number (4–7) of deoxyribonucleotide residues (underlined). The RNA RT and RT3P are as defined in Table 1. The mismatched base is shown in boldface.
[b]T_m determined from curve fits of the UV absorbance versus temperature profiles using a two-state transition model.
[c]$\Delta T_m = T_m$ (mismatched duplex) $- T_m$(matched duplex).

DNA window in the MBOs, we hoped to restrict RNase H binding and cleavage to a confined site over the single mismatch of the MBO·RNA duplex.

Under the experimental conditions, approximately 80% cleavage of the matched RNA target (RT) resulted when the control ODN hybridized to the target RNA. Autoradiograms of denaturing PAGE fractionations of RNase H digested target RNAs are shown in Figures 2(A), 3(A), and 4(A). The presence of the slower mobility bands and smears above the intact RNA bands in the autoradiograms indicates that some of the MBOs formed complexes with the intact RNA targets under denaturing conditions of PAGE experiments. The occurrence and intensity of the MBO·RNA complex bands correlated well with the T_ms of the corresponding duplexes (see Tables 2–4). The autoradiograms also revealed that MBOs containing four or more DNA residues in the M-construct or five or more DNA residues in the 3P-construct supported RNase H cleavage of the matched targets under the experimental conditions.[3,9,12,19] The MBOs containing four or more DNA residues in the 5P-construct also activated RNase H for target cleavage, in contrast to an earlier report.[19] This discrepancy could be due to the fact that the RNA target used in the previous study was not of sufficient length to effect RNase H binding to that particular substrate for cleavage. We used RNA targets with additional ribonucleotides flanking the hybridization region with MBOs, whereas the previous study used

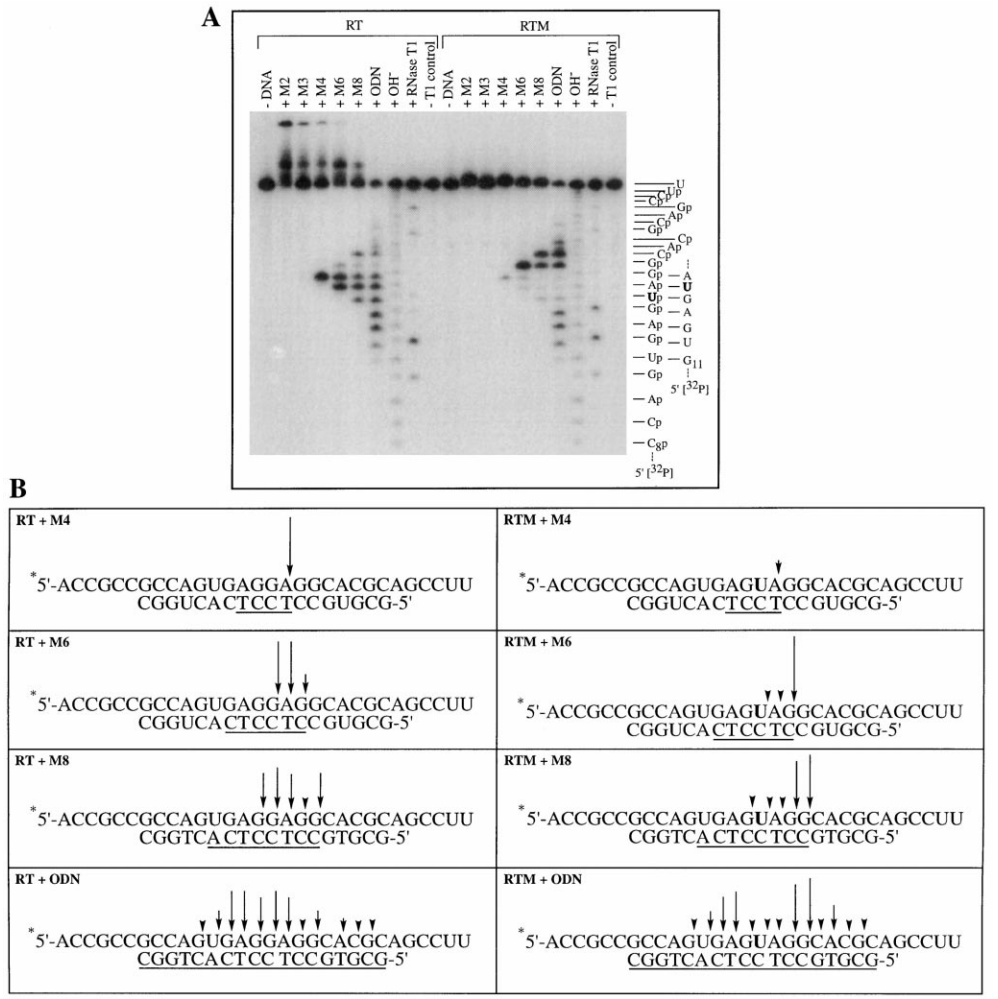

Figure 2. (A) RNase H digestion pattern of 5′-^{32}P-labeled RNA targets RT and RTM hybridized to MBOs M2 through M8 or to control ODN: -DNA, control RNA lane without any oligonucleotide added; -OH-, alkaline hydrolysis reaction; + RNase T1, RNase T1 digestion reaction; -T1 control, control lane without RNase T1 added. Alignment of RNA bands with ribonucleotide sequence is shown for RNA RTM; the mismatched base is shown in boldface. (B) Schematic representation of RNase H cleavage sites.

RNA targets of the same length of the antisense oligonucleotides. Unlike the results of another earlier report, however, we did not observe RNase H cleavage in the single-stranded region of the target RNA extending 3′- from the ODN or MBO·RNA heteroduplex[26] except for 5P-set of MBOs. Even in this case the RNase H cleavage extended only one nucleotide into the 3′-single-stranded region with the singly-mismatched RNA target (RT3P) (see Fig. 4(B)). A recent study by Lapham et al. showed that *E. coli* RNase H cleavage position on RNA is dependent on the enzyme source.[27] We have used RNase H obtained from Pharmacia in the present study, whereas Lima and Crooke[26] used the enzyme obtained from USB. This difference in the enzyme source may partly account for the difference in the cleavage of the 3′ overhang region of RNA as observed by the two groups.

In order to identify the exact sites of RNase H cleavage in the RNA targets, the single cleavage product band in the M4 + RT lane (see Fig. 2) was cut out and extracted from the gel by passive elution and ethanol precipitated. The size and sequence of the extracted RNA cleavage product were confirmed by alkaline hydrolysis and RNase T1 digestion experiments (data not shown). The single 5′-^{32}P-labeled RNA fragment in the M4 + RT lane corresponded to an RNase H cleavage at the A17pG18 dinucleotide junction of the target complementary to

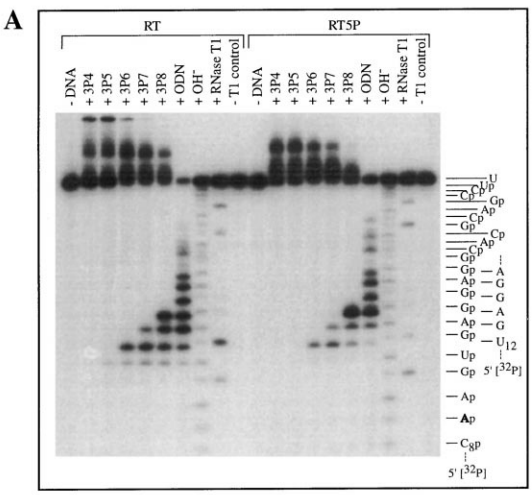

B

RT + 3P5 *5'-ACCGCCGCCAGUGAGGAGGCACGCAGCCUU CGGTCACUCCUCCGUGCG-5'	**RT5P + 3P5** *5'-ACCGCCGCAAGUGAGGAGGCACGCAGCCUU CGGTCACUCCUCCGUGCG-5'
RT + 3P6 *5'-ACCGCCGCCAGUGAGGAGGCACGCAGCCUU CGGTCACUCCUCCGUGCG-5'	**RT5P + 3P6** *5'-ACCGCCGCAAGUGAGGAGGCACGCAGCCUU CGGTCACUCCUCCGUGCG-5'
RT + 3P7 *5'-ACCGCCGCCAGUGAGGAGGCACGCAGCCUU CGGTCACUCCUCCGUGCG-5'	**RT5P + 3P7** *5'-ACCGCCGCAAGUGAGGAGGCACGCAGCCUU CGGTCACUCCUCCGUGCG-5'
RT + 3P8 *5'-ACCGCCGCCAGUGAGGAGGCACGCAGCCUU CGGTCACTCCUCCGUGCG-5'	**RT5P + 3P8** *5'-ACCGCCGCAAGUGAGGAGGCACGCAGCCUU CGGTCACTCCUCCGUGCG-5'
RT + ODN *5'-ACCGCCGCCAGUGAGGAGGCACGCAGCCUU CGGTCACTCCTCCGTGCG-5'	**RT5P + ODN** *5'-ACCGCCGCAAGUGAGGAGGCACGCAGCCUU CGGTCACTCCTCCGTGCG-5'

Figure 3. (A) RNase H digestion pattern of 5′-^{32}P-labeled RNA targets RT and RT5P hybridized to MBOs 3P4 through 3P8 or to control ODN: -DNA, control RNA lane without any oligonucleotide added; -OH-, alkaline hydrolysis reaction; + RNase T1, RNase T1 digestion reaction; -T1 control, control lane without RNase T1 added. Alignment of RNA bands with ribonucleotide sequence is shown for RNA RTM; the mismatched base is shown in boldface. (B) Schematic representation of RNase H cleavage sites.

the C7(2′-*O*-methyl)pT8(2′-deoxy) sequence of MBO, M4. This allowed a correct alignment of RNase H-digested RNA bands (RNA fragments with a 3′-OH group) with alkaline-hydrolyzed or T1 digested RNA bands (RNA fragments with a 2′-3′-cyclic phosphate) in the autoradiograms (Figs 2(A), 3(A), and 4(A)), thus allowing precise determination of RNase H cleavage sites in the RNA target (Figs 2(B), 3(B), and 4(B)).

As predicted, the incorporation of non-RNase H activating 2′-*O*-methylribonucleotides into the 18-mer antisense oligonucleotide reduced the number of cleavage sites in the target RNAs, thus enhancing the cleavage site specificity on a single target. In the presence of the matched target, the number of cleavage sites reduced from more than 10 sites for the control ODN to 2–4 sites for MBOs with a six-base DNA segment, and to only one or two sites for MBOs with a four-base DNA segment.

Densitometric analyses of percent cleavages of the complementary and mismatched RNA targets suggest that the M- and 3P-sets of the MBOs were less active in inducing RNase H cleavage of the matched RNA target (RT) than the control ODN (Fig. 5), in agreement with previous reports of RNase H activation properties of 2′-*O*-methyl/deoxyribonucleotide containing MBOs.[9,12]

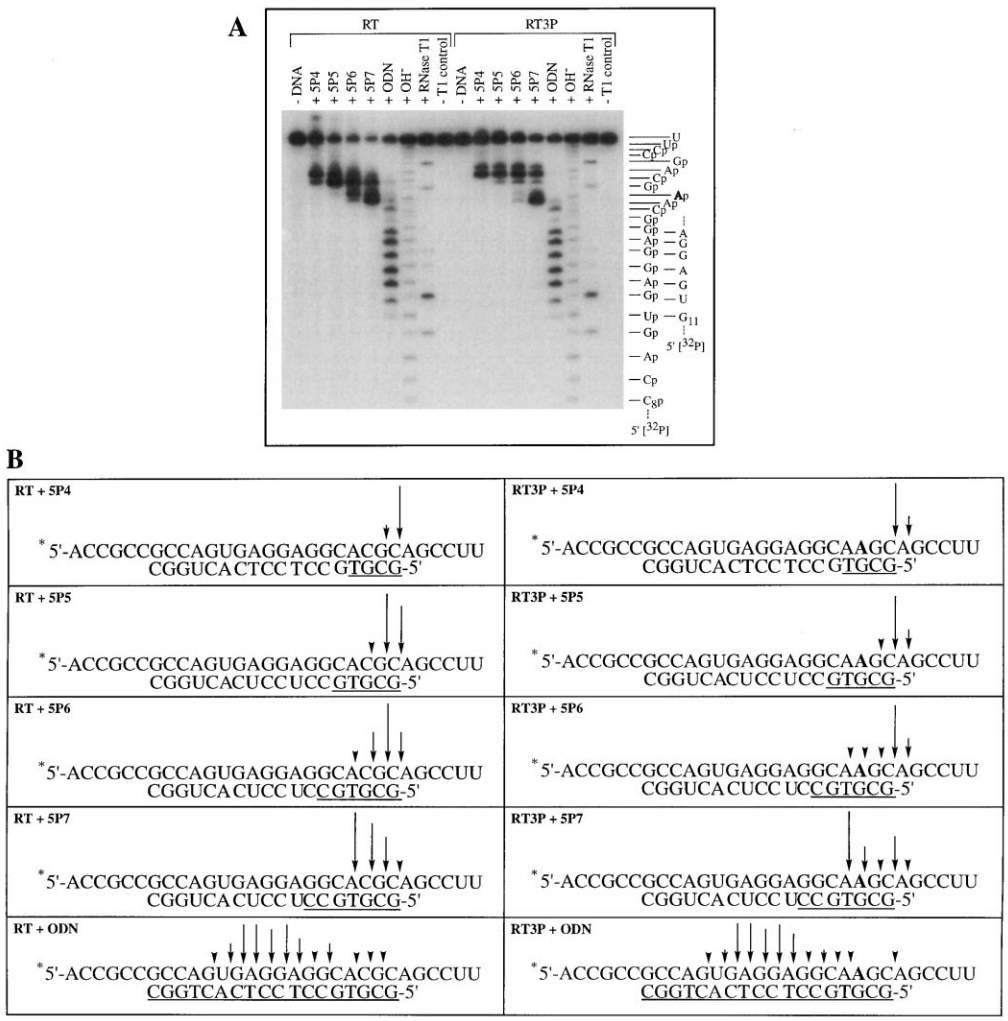

Figure 4. (A) RNase H digestion pattern of 5′-^{32}P-labeled RNA targets RT and RT3P hybridized to MBOs 5P4 through 5P7 or to control antisense ODN: -DNA, control RNA lane without any oligonucleotide added; -OH-, alkaline hydrolysis reaction; + RNase T1, RNase T1 digestion reaction; -T1 control, control lane without RNase T1 added. Alignment of RNA bands with ribonucleotide sequence is shown for RNA RTM; the mismatched base is shown in boldface. (B) Schematic representation of RNase H cleavage sites.

Two of the 5P-set MBOs (5P6 and 5P7) have RNase H-dependent target cleaving capabilities within ±3% of the control ODN, however, despite their shortened DNA segments. These results are consistent with the previously proposed mechanism of *E. coli* RNase H digestion of RNA in the DNA·RNA hybrid duplex region.

Selectivity of the MBOs for the target RNAs was assessed by comparing percent RNA cleavage of the matched and singly mismatched RNA targets for the MBOs and control ODN (Fig. 5). Among all MBOs examined, M4, which contains four deoxyribonucleoside residues flanked on each side by seven 2′-*O*-methylribonucleosides, showed higher point mutation selectivity while maintaining a moderate cleavage efficiency in the matched target.

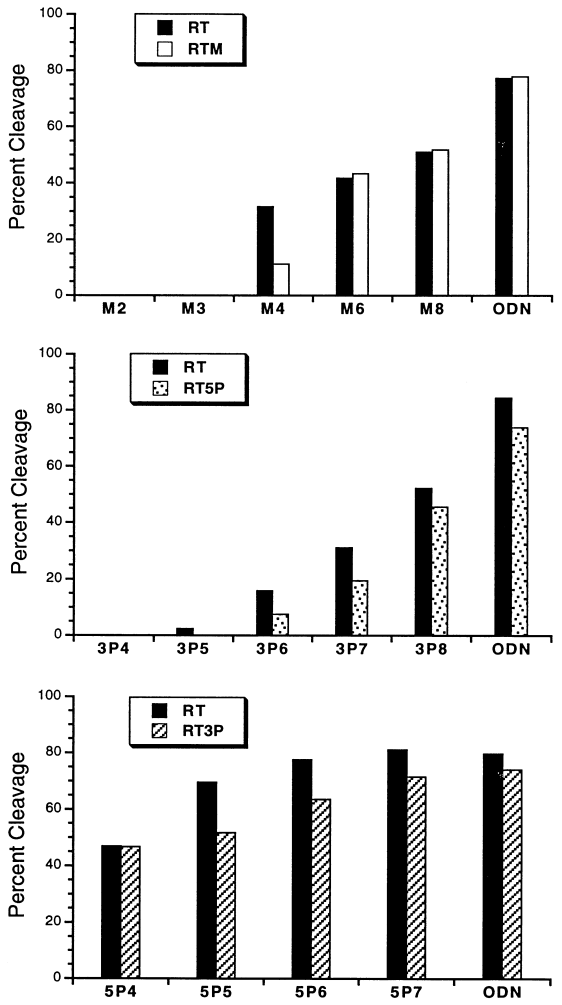

Figure 5. Percent target RNA cleavage by RNaseH in the presence of MBOs and control ODN.

Discussion

In vitro and in vivo stability, and tissue disposition of PS-MBOs containing DNA and 2′-*O*-methyl RNA segments have been well established.[10,12] Previous studies showed that MBOs of type M- and 5P-sets are more stable towards nucleolytic enzymes than PS-ODNs and 3P-set MBOs.[12] The present study is aimed at understanding the target binding affinity and specificity, and point mutation selectivity of MBOs in vitro.

The UV absorbance melting studies on the MBO·RNA binding equilibrium have suggested that the partial incorporation of 2′-*O*-methylribonucleosides in antisense oligonucleotides increases the thermodynamic stability of MBO·RNA heteroduplexes. When targeted to the same set of matched and singly mismatched RNA targets, the MBOs show reduced differential binding affinity (less negative ΔT_m) than the control ODN. The difference in ΔT_m between the duplexes of MBOs and the duplex of control ODN is sensitive to the position of the mismatched base in the target. A greater difference in ΔT_m (~9 °C) was observed when the mismatched base position is near the 3′-end of the RNA sequence (RT3P). The UV melting measurements acquired on each of the RNA targets alone indicated that the matched target RT and singly mismatched target RT3P formed secondary structures that melted at approximately 70 °C (data not shown). Partial T1 digestion experiments performed on these RNA targets revealed the same cleavage pattern for RT and RT3P, and both RNA sequences had the same G residues inaccessible for T1 digestion at 55 °C (Fig. 4). These results suggest that RT and RT3P formed similar secondary structures, most likely hairpins containing a six-base-pair stem (including a G·A pair) and an AGUGA pentaloop. The presence of stable secondary structures in RNA targets can directly influence the target binding specificity of a hybridizing oligonucleotide.[28,29] The control ODN bound less strongly to the mismatched target RT3P, which forms a hairpin structure ($\Delta T_m = -13.7$ °C) than to RT5P ($\Delta T_m = -4.7$ °C). However, when the binding affinities of the MBOs for both the matched and the mismatched targets were greatly enhanced by 2′-*O*-methyl modifications, such as in the case of 5P-set MBOs binding to RT and RT3P, the influence of RNA secondary structure on binding specificity of MBOs was diminished (ΔT_m −4 °C as compared to −13.7 °C for control ODN). Among MBO·RNA duplexes studied, the destabilization effect by a single mismatch was greater when the mismatch was in the middle than near the ends of the target sequence, as determined by UV melting experiments. Because of high affinities of these MBOs for the RNA targets, however, the observed global destabilization of the MBO·RNA duplexes by a single mismatch was

insignificant, and the target binding specificity was not improved over ODN.

Previous studies have shown that RNase H induces an endonucleolytic cleavage near the 3′-terminus of the RNA strand in a DNA·RNA heteroduplex, then processively and exonucleolytically degrades the RNA.[3,19] The initial cleavage by RNase H near the 3′-end of the matched target RT in the MBO·RT heteroduplex should not be greatly affected by 2′-*O*-methyl modification at the 3′-half of the MBO, provided that a complete hybridization of the target is achieved with either 2′-*O*-methyl-modified or unmodified oligonucleotide. This could explain the high efficiency of RNA cleavage for some of the 5P-set MBOs. The efficiency of RNA cleavage reduces in the order of 3P-set < M-set < 5P-set of MBOs with the same DNA window size. This result further suggests that initial binding of RNase H occurs near the 3′-end (with respect to the RNA target) of MBO·RNA heteroduplex and that the location of this initial binding site is not influenced by the 2′-*O*-methyl modification in the MBO strand of the duplex. The bound RNase H then either initiates a cleavage when bound to a DNA·RNA hybrid region or scans in a 3′–5′ direction (with respect to the RNA target) until it reaches a DNA·RNA hybrid region to effect a cleavage.

Higher target binding specificity of antisense oligonucleotides is crucial in achieving single base discrimination.[30–32] Whereas, our approach aimed at defining a minimum substrate cleavage site for RNase H such that a single point mutation within the cleavage site would not be tolerated even when the mismatched target is tightly bound by an MBO. With *E. coli* RNase H, the minimum substrate cleavage site discriminatory for a single point mutation has been identified to be four DNA·RNA base pairs sandwiched by non-RNase H activating 2′-*O*-methyl RNA·RNA regions (M4) or five to six DNA·RNA base pairs flanked on the 3′ side (with respect to the RNA target) by non-RNase H activating 2′-*O*-methyl RNA·RNA base pairs (3P5 and 3P6). Greater than 50% difference in target cleavage efficiencies between the matched and singly mismatched targets has been obtained with these MBOs of improved selectivity over the control ODN. Contrary to the 3P-set MBOs, the 5P-set MBOs, with their target-cleaving domain containing five or more DNA residues located at the 5′-end of the antisense sequence, are highly efficient in inducing RNase H cleavage as compared to the control ODN even when hybridized to the point-mutated target. MBOs with 5P-set backbone constructs are therefore not suitable for targeting single point mutations.

In conclusion, the present study suggests the following: (i) *E. coli* RNase H recognizes the DNA·RNA heteroduplex, binds and initiates an endonucleolytic cleavage near the 3′-terminus of the RNA strand in the heteroduplex region, and then processively and exonucleolytically digests the RNA strand in the duplex region; (ii) incorporation of 2′-*O*-methylribonucleotide residues in antisense oligonucleotides increases affinity of the MBO for the target RNA; (iii) the number and position of the DNA residues in the MBOs influence both affinity for the target and selectivity of the RNase H cleavage, (iv) the RNase H cleavage confines to the ODN·RNA heteroduplex region and does not extend into the 3′- single-stranded overhanging region of the RNA target (with the enzyme used in this study), and (v) the placement of five or more DNA residues at the 5′-end of the MBO (5P-set) activates RNase H to a greater extent than in the other positions (M- and 3P-sets) of the MBO. Since both the restriction of RNase H cleavage site and the enhancement of target binding specificity can modulate point mutation selectivity of MBOs, further improvement of MBOs for targeting single point mutations could be made by properly reducing the length of the 2′-*O*-methylribonucleotide segments in the flanking region. It would be unreasonable to extrapolate these model studies to eukaryotic systems in the absence of well characterized eukaryotic RNase H studies.

Experimental

Oligonucleotide synthesis and purification

2′-*O*-Methyl/deoxyribonucleotide MBO phosphorothioates and phosphodiester target oligoribonucleotides (RNAs) were chemically synthesized as described previously.[12] Crude MBOs were purified by reverse-phase HPLC on a C18 column and were subsequently detritylated with 80% acetic acid. Crude RNAs were purified by denaturing polyacrylamide gel electrophoresis (PAGE) on 20% gels. Full-length RNAs were passively eluted from the gel and ethanol precipitated. The HPLC or gel purified oligonucleotides were desalted by dialysis against deionized water for 48 h with four changes of water. The concentrations of the MBOs and target RNAs were determined by UV absorbance measurements at 260 nm using extinction coefficients calculated by the nearest neighbor method.[33]

UV absorbance melting experiments

MBOs and RNA targets were mixed at 1:1 molar ratio, dried in a speed vac and resuspended in a buffer containing 100 mM NaCl, 0.1 mM Na_2EDTA, 10 mM sodium phosphate, pH 7.4. In each sample, the total oligonucleotide strand concentration was 2 μM in a total volume of 1 mL. The samples were heated at 85 °C for 2 min and cooled at room temperature for 20 min

prior to UV absorbance melting measurements. UV absorbance melting curves were recorded at 260 nm using a GBC Model 920 spectrophotometer equipped with a 6-by-1 or a 6-by-6 Peltier-effect cell holder controlled by an external Thermocell. The samples were heated at a rate of 0.5 °C/min. Data were recorded on a QUANTEX personal computer interfaced with the spectrophotometer and processed using KaleidaGraph 3.0 on a Power Macintosh computer. The melting temperatures (T_m) of the duplexes were determined from curve fits of the melting profiles using a two-state transition model.[33,34] The reproducibility of the T_m values was within ± 0.5 °C.

End labeling of RNA

Purified RNAs were ^{32}P-labeled at 5′-end using T4 polynucleotide kinase (Pharmacia) and γ-^{32}P-ATP (Amersham). Fifty picomoles of RNA were mixed with 20 μCi γ-^{32}P-ATP and 29 U of T4 kinase and incubated at 37 °C for 30 min in 20 μL buffer containing 20 mM $MgCl_2$, 50 mM HEPES at pH 8.1. At the end of the incubation, reaction mixture was mixed with 179 μL TE buffer (10 mM Tris, 1 mM Na_2EDTA, pH 7.5) and 1 μL of phenol extracted 10 μg/μL glycogen, and extracted three times with phenol (pH 8) and once with chloroform/isoamylalcohol (24/1). The labeled RNA in the aqueous phase was subsequently ethanol precipitated. The RNA pellet was washed once with 70% ethanol, dried in a speed vac for 5 min and resuspended in 100 μL autoclaved deionized water.

RNase H digestion assay

Hybridization of MBOs (330 nM) and the end-labeled RNA target (33 nM) was carried out in 15 μL buffer containing 10 mM KCl, 5 mM $MgCl_2$, 0.1 mM DTT, 5% glycerol, 20 mM Tris–HCl at pH 7.5 and 10 μg phenol-extracted glycogen. The mixture was heated at 85 °C for 1 min, cooled at room temperature for 5 min and incubated at 37 °C for 5 min. RNase H digestion was initiated by adding 0.08 U of *E. coli* RNase H (Pharmacia) followed by incubation at 37 °C for 10 min. The reaction was stopped by adding 20 μL gel loading dye (0.017% xylene cyanol and 0.017% bromophenol blue in formamide) and freezing at −70 °C. RNase T1 digestion was carried out at 55 °C for 1 min in 15 μL of buffer containing 50 mM KCl, 5 mM $MgCl_2$, 25 mM NaOAc, pH 5.2 in the presence of 1 pmol 5′-^{32}P-RNA, 3 μg carrier tRNA, and 0.01 U RNase T1 (Pharmacia). The cleavage products were fractionated on 20% denaturing polyacrylamide gels, and the cleavage patterns visualized by autoradiography. The percent cleavage of RNA targets was analyzed by densitometry. Film exposure was controlled such that the band intensities were within the linear range of densitometric measurements.

Acknowledgements

The authors would like to thank Ms. Adrienne Manning for excellent technical assistance and Dr Wenqiang Zhou for the synthesis of some of the RNA RT.

References and Notes

1. Walder, R. Y.; Walder, J. A. *Proc. Natl. Acad. Sci. U.S.A.* **1988**, *85*, 5011.

2. Furdon, P. J.; Dominski, Z.; Kole, R. *Nucl. Acids Res.* **1989**, *17*, 9193.

3. Agrawal, S.; Maynard, S. H.; Zamecnik, P. C.; Pederson, T. *Proc. Natl. Acad. Sci. U.S.A.* **1990**, *87*, 1401.

4. Woolf, T. M.; Jennings, C. G.; Rebagliati, M.; Melton, D. A. *Nucl. Acids Res.* **1990**, *18*, 1763.

5. Young, S.; Wagner, R. W. *Nucl. Acids Res.* **1991**, *19*, 2463.

6. Monia, B. P.; Lesnik, E. A.; Gonzalez, C.; Lima, W. F.; McGee, D.; Guinosso, C. J.; Kawasaki, A. M.; Cook, P. D.; Freier, S. M. *J. Biol. Chem.* **1993**, *268*, 14514.

7. Gao, W.-Y.; Han, F.-S.; Storm, C.; Egan, W.; Cheng, Y.-C. *Mol. Pharmacol.* **1992**, *41*, 223.

8. Agrawal, S. *Trends Biotech.* **1992**, *10*, 152.

9. Metelev, V.; Lisziewicz, J.; Agrawal, S. *Bioorg. Med. Chem. Lett.* **1994**, *4*, 2929.

10. Zhang, R.; Lu, Z.; Zhao, H.; Zhang, X.; Diasio, R. B.; Habus, I.; Jiang, Z.; Iyer, R. P.; Yu, D.; Agrawal, S. *Biochem. Pharmacol.* **1995**, *50*, 545.

11. McKay, R. A.; Cummins, L. L.; Graham, M. J.; Lesnik, E. A.; Owens, S. R.; Winniman, M.; Dean, N. M. *Nucl. Acids Res.* **1996**, *24*, 411.

12. Agrawal, S.; Jiang, Z.; Zhao, Q.; Shaw, D.; Cai, Q.; Roskey, A.; Channavajjala, L.; Saxinger, C.; Zhang, R. *Proc. Natl. Acad. Sci. U.S.A.* **1997**, *94*, 2620.

13. Baker, B. F.; Lot, S. S.; Condon, T. P.; Cheng-Flournoy, S.; Lesnik, E. A.; Sasmor, H. M.; Bennett, C. F. *J. Biol. Chem.* **1997**, *272*, 11994.

14. Kandimalla, E. R.; Manning, A.; Zhao, Q.; Shaw, D. R.; Byrn, R. A.; Sasisekharan, V.; Agrawal, S. *Nucl. Acids Res.* **1997**, *25*, 370.

15. Agrawal, S.; Goodchild, J. *Tetrahedron Lett.* **1987**, *28*, 3539.

16. Giles, R. V.; Tidd, D. M. *Nucl. Acids Res.* **1992**, *20*, 763.

17. Giles, R. V.; Ruddell, C. J.; Spiller, D. G., Green, J. A.; Tidd, D. M. *Nucl. Acids Res.* **1995**, *23*, 954.

18. Hogrefe, H. H.; Hogrefe, R. I.; Walder, R. Y.; Walder, J. A. *J. Biol. Chem.* **1990**, *265*, 5561.

19. Crooke, S. T.; Lemonidis, K. M.; Neilson, L.; Griffey, R.; Lesnik, E. A.; Monia B. P. *Biochem. J.* **1995**, *312*, 599.

20. Lima, W. F.; Crooke, S. T. *Biochemistry* **1997**, *36*, 390.

21. Inoue, H.; Hayase, Y.; Iwai, S.; Ohtsuka, E. *FEBS Lett.* **1987**, *215*, 327.

22. Kandimalla, E. R.; Venkataraman, G.; Sasisekharan, V.; Agrawal, S. *J. Biomol. Struct. Dyn.* **1997**, *14*, 715.

23. Nishizaki, T.; Iwai, S.; Ohtsuka, E.; Nakamura, H. *Biochemistry* **1997**, *36*, 2577.

24. Blommers, M. J. J.; Pieles, U.; Mesmaeker, A. D. *Nucleic Acids Res.* **1994**, *22*, 4187.

25. Leslie, A.G.W.; Arnott, S. *J. Mol. Biol.* **1978**, *119*, 399.

26. Lima, W. F.; Crooke, S. T. *J. Biol. Chem.* **1997**, *272*, 27513.

27. Lapham, J.; Yu, Y.-T.; Shu, M.-D.; Steitz, J. A.; Crothers, D. M. *RNA* **1997**, *3*, 950.

28. Goodchild, J.; Agrawal, S.; Civeira, M. P.; Sarin, P. S.; Sun, D.; Zamecnik, P. C. *Proc. Natl. Acad. Sci. U.S.A.* **1988**, *85*, 5507.

29. Freier, S. M. In *Antisense Research and Application*; Crooke, S. T.; Lebleu, B., Eds.; CRC: Boca Raton, 1993; pp 67–82.

30. Larrouy, B.; Boiziau, C.; Sproat, B.; Toulme, J.-J. *Nucl. Acids Res.* **1995**, *23*, 3434.

31. Larrouy, B.; Blonski, C.; Boiziau, C.; Stuer, M.; Moreau, S.; Shire, D.; Toulme, J.-J. *Gene* **1992**, *121*, 189.

32. Duroux, I.; Godard, G.; Boidot-Forget, M.; Schwab, G.; Helene, C.; Saison-Behmoaras, T. *Nucl. Acids Res.* **1995**, *23*, 3411.

33. Puglisi, J. D.; Tinoco, Jr. I., *Meth. Enzymol.* **1989**, *180*, 304.

34. Marky, L. A.; Breslauer, K. J. *Biopolymers* **1987**, *26*, 1601.